scientific reports

Check for updates

OPEN

Dissecting the roles of Haspin and VRK1 in histone H3 phosphorylation during mitosis

Tyrell N. Cartwright[1,6], Rebecca J. Harris[1,6], Stephanie K. Meyer[1], Aye M. Mon[2,3], Nikolaus A. Watson[1], Cheryl Tan[1], Agathe Marcelot[4], Fangwei Wang[5], Sophie Zinn-Justin[4], Paula Traktman[2,3] & Jonathan M. G. Higgins[1]✉

Protein kinases that phosphorylate histones are ideally-placed to influence the behavior of chromosomes during cell division. Indeed, a number of conserved histone phosphorylation events occur prominently during mitosis and meiosis in most eukaryotes, including on histone H3 at threonine-3 (H3T3ph). At least two kinases, Haspin and VRK1 (NHK-1/ballchen in *Drosophila*), have been proposed to carry out this modification. Phosphorylation of H3 by Haspin has defined roles in mitosis, but the significance of VRK1 activity towards histones in dividing cells has been unclear. Here, using in vitro kinase assays, KiPIK screening, RNA interference, and CRISPR/Cas9 approaches, we were unable to substantiate a direct role for VRK1, or its paralogue VRK2, in the phosphorylation of threonine-3 or serine-10 of Histone H3 in mitosis, although loss of VRK1 did slow cell proliferation. We conclude that the role of VRKs, and their more recently identified association with neuromuscular disease and importance in cancers of the nervous system, are unlikely to involve mitotic histone kinase activity. In contrast, Haspin is required to generate H3T3ph during mitosis.

The structure and function of chromosomes undergo radical changes during cell division, including chromosome condensation, downregulation of gene expression, removal of cohesion between chromosomes, and the assembly of kinetochores at centromeres to drive chromosome segregation. Protein kinases are instrumental in bringing about these alterations, and kinases that act directly on histones are well-placed to influence the behavior of chromatin. Indeed, a number of histone phosphorylation events occur prominently during mitosis and meiosis in most eukaryotes including yeasts, plants and animals[1]. Among these are phosphorylation of histone H3 at threonine-3 (H3T3ph) and serine-10 (H3S10ph), and histone H2A at threonine-120 (H2AT120ph; or the equivalent H2AT119ph in *Drosophila*). For example, in mammalian cells, H3T3ph first becomes detectable at foci on chromosome arms in early prophase, concentrates most strongly at inner centromeres in prometaphase and metaphase, and declines during anaphase[2,3]. A key function of H3T3ph is to position the Chromosomal Passenger Complex (CPC) correctly at inner centromeres[4–6]. The CPC contains the kinase Aurora B that regulates chromosome segregation by modulating the phosphorylation status of a number of centromere and kinetochore substrates[7]. In addition, H3T3ph may participate in a phospho-methyl switch to prevent histone reading proteins such as the transcription factor TFIID from binding to the adjacent modification H3K4me3 during mitosis[8].

Central to understanding the role of any histone phosphorylation event is knowledge of the kinases responsible. Two kinases have been proposed to carry out phosphorylation of H3T3 during mitosis. One of these is Haspin, an atypical kinase (encoded by Germ cell Specific Gene-2, GSG2) that phosphorylates H3 peptides, recombinant H3, and nucleosomes, specifically at threonine-3 in vitro[9,10]. Haspin RNAi, inhibitors, or CRISPR/Cas9 targeting all remove mitotic H3T3ph in cultured mammalian cells, supporting the view that this is a critical kinase for H3T3ph during cell division[9,11–14]. Loss or inhibition of Haspin impairs chromosome alignment and segregation in cell culture[9,12,15], particularly when cells are transiently blocked in mitosis[14], or when another

[1]Biosciences Institute, Faculty of Medical Sciences, Newcastle University, Framlington Place, Newcastle upon Tyne NE2 4HH, UK. [2]Department of Biochemistry and Molecular Biology, Medical University of South Carolina, Charleston, SC 29425, USA. [3]Department of Microbiology and Immunology, Medical University of South Carolina, Charleston, SC 29425, USA. [4]Institute for Integrative Biology of the Cell (I2BC), CEA, CNRS, Université Paris-Sud, Université Paris-Saclay, Gif-sur-Yvette Cedex, France. [5]MOE Laboratory of Biosystem Homeostasis and Protection, Innovation Center for Cell Signaling Network, Life Sciences Institute, Zhejiang University, Hangzhou, Zhejiang, China. [6]These authors contributed equally: Tyrell N. Cartwright and Rebecca J. Harris. ✉email: jonathan.higgins@ncl.ac.uk

kinase that helps recruit Aurora B to centromeres, Bub1, is also inhibited[16,17]. Bub1 may compensate for the loss of Haspin by producing H2AT120ph, which can indirectly recruit the CPC to centromeres[6,16–18].

Other work, however, has implicated Vaccinia-Related Kinase-1 (VRK1) as a mitotic H3T3 kinase[19–25], a concept that has been broadly reported[26–41] and incorporated into databases such as Ingenuity and BioGRID, influencing the structure of proposed biological networks[42,43]. VRK1 is a member of a subgroup of the Casein Kinase-1 (CK1) family that also contains VRK2 and the pseudokinase VRK3[44], and it has proposed roles in regulation of a number of transcription factors, the DNA damage response, and nuclear envelope remodeling during mitosis[36,45]. In addition, VRK1 is reported to phosphorylate H3T3 in vitro[19–23,25,46], and VRK1 RNAi can diminish H3T3ph in mammalian cells[19,21,23,26]. In some reports, but not others, VRK1 is also able to phosphorylate H3S10 in vitro, and to influence H3S10ph in cells[19–21,23,26,47]. For example, infection of gastric epithelial cells with *Helicobacter pylori* was found to reduce H3T3ph and H3S10ph, and this could be rescued by overexpression of VRK1[24]. VRK1 overexpression causes nuclear condensation, leading to the suggestion that H3T3ph (and H3S10ph) are major regulators of chromosome condensation during mitosis[19], a model that has been widely disseminated[23,25,27–36].

The relative roles of Haspin and VRK1 in H3T3 phosphorylation remain to be defined. Some authors find that both VRK1 and Haspin are required for full H3T3ph in mitotic cells[21,26]. Others have proposed that VRK1 is essential to trigger generalized H3T3ph in early mitosis, and that Haspin acts only later in mitosis. In this model, VRK1 phosphorylates H3T3ph to condense chromosomes and recruit the CPC, and Aurora B then activates Haspin to generate localized H3T3ph at centromeres[23,36]. This work contrasts with other models in which the timing and location of H3T3ph is controlled indirectly by Cdk1, Bub1, Plk1 and Aurora kinases acting through Haspin and the H3T3ph phosphatase Repo-Man/PP1[48–54]. VRK1 mutations in humans appear to cause neurodegenerative disorders[30,55,56] and, consistent with this, VRK1$^{GT3/GT3}$ hypomorphic mice have reduced brain weight and mild motor dysfunction[57]. Significantly, VRK1 has been identified recently as a compelling synthetic lethal target in nervous system cancers with low expression of VRK2[41,58]. These findings reinforce the need to understand the molecular functions of VRK1. In this study, we use a variety of methods, including a new kinase screening approach, to clarify the contribution of Haspin and VRK1 to H3T3ph and chromosome condensation in mitosis.

Results

Recombinant Haspin phosphorylates H3T3 more efficiently than VRK1 in vitro. To compare the activity of human Haspin and human VRK1 towards Histone H3T3, we conducted in vitro kinase assays using recombinant Haspin (residues 471–798), recombinant full-length VRK1, and peptides corresponding to the first 21 amino acids of H3. Three different preparations of recombinant VRK1, produced in both *E. coli* or in Sf9 insect cells, were similarly able to weakly phosphorylate H3(1–21) at the high concentration of 10 nM. However, Haspin generated H3T3ph more strongly than VRK1, even at 0.1 nM (Fig. 1A). VRK1 has been reported to phosphorylate nucleosomes more effectively than free histones[59], so we also compared the activity of Haspin and VRK1 on purified recombinant nucleosomes. In this case, Haspin but not VRK1 was able to phosphorylate H3T3 (Fig. 1B). Recombinant VRK1 was active on its well-established substrate, residue S4 of Barrier-to-Autointegration Factor (BAF)[41,45,58,60–64] (Supplementary Fig. 1). Therefore, in these in vitro assays, Haspin was at least 100-fold more active towards H3T3 than was VRK1.

Furthermore, when we directly compared the ability of various forms of recombinant human VRK1 to phosphorylate recombinant human BAF or Histone H3 using [γ^{32}P]-ATP incorporation assays, BAF was clearly the preferred substrate (Fig. 1C). Indeed, only GST-VRK1, but neither 3xFLAG-VRK1 nor His-VRK1, had any detectable activity towards Histone H3. Notably, GST-VRK1 lost the ability to phosphorylate H3 when the GST tag was removed, while BAF phosphorylation was unaffected (Fig. 1C). Therefore, VRK1 consistently phosphorylated BAF but not H3 in vitro.

A kinase activity screen implicates Haspin, not VRKs, as the mitotic H3T3 kinase. Recombinant kinases may lack cofactors (such as post-translational modifications or activating subunits) that are required for activity towards their substrates. To identify H3T3 kinases in a more physiological environment, and in an unbiased fashion, we made use of a new kinase screening methodology known as KiPIK (Kinase inhibitor Profiling to Identify Kinases) that uses cell extracts as a source of kinases[65]. The method compares the pattern of inhibition of the unknown kinase activity in cell extracts with the inhibition profiles of known protein kinases determined in vitro using small molecule kinase inhibitors. We determined which kinase(s) in mitotic HeLa cell extract were able to phosphorylate H3(1–21) peptides, detected with anti-H3T3ph antibodies. We used HeLa cells because VRK1 was originally reported to be crucial for H3T3ph in this cell type[19]. To generate an inhibition fingerprint for H3T3 kinase activity in extract, we used a library of 140 kinase inhibitors that have been profiled on numerous purified kinases in vitro (Supplementary Data 1). This included 84 of the 178 inhibitors profiled at 0.5 μM on 300 kinases by Anastassiadis et al.[66], and 63 of the 158 inhibitors profiled at 1 μM or 10 μM on 234 kinases by Gao et al.[67], all using conventional in vitro kinase assays. In addition, it included all 72 inhibitors profiled on 388 different kinases by Davis et al. using the DiscoverX competition binding assay[68], and 50 of the 156 inhibitors tested at 10 μM for binding to 60 kinases by Federov et al. using a thermal denaturation assay[69]. Together, this incorporates 444 kinases (405 unique human kinase genes; Supplementary Data 2).

The results showed that, in every case where Haspin was present in the profiling dataset, it was the top hit in the screen (Fig. 2A–E, red circles). By contrast, no VRK kinase scored within the top 40% of kinases (Fig. 2A–E, blue circles). Indeed, with the exception of the Anastassiadis screen (where VRK1 was 126th out of 300 kinases), VRK1, VRK2 and VRK3 were all found in the bottom 20% of kinases (Fig. 2A–E; Supplementary Data 3). These results are consistent with previous KiPIK screens for H3T3 kinases[65], where Haspin was the top overall hit, but

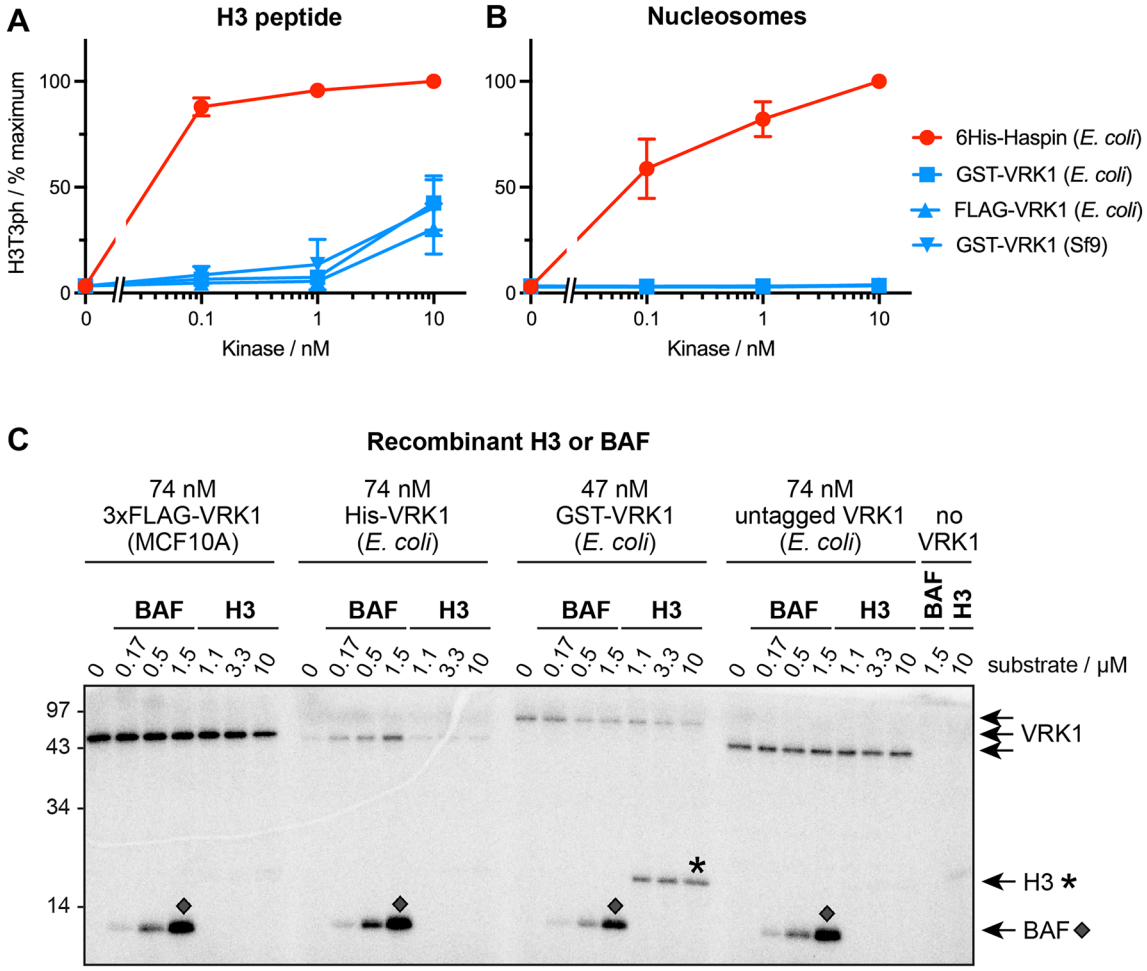

Figure 1. Phosphorylation of Histone H3 and BAF by recombinant human Haspin or VRK1. Phosphorylation of H3T3 by Haspin and VRK1 on (**A**) H3(1–21) peptides, and (**B**) recombinant nucleosome substrates, detected by H3T3ph antibodies. Error bars show means ± SD, n = 3 independent experiments. In (**C**), phosphorylation of recombinant BAF or H3 by various preparations of recombinant VRK1 were monitored by [γ^{32}P]-incorporation, SDS-PAGE and phosphorimaging analysis. The integrity and purity of the proteins was validated by SDS-PAGE and silver-staining. The original gel is presented in Supplementary Fig. 7.

VRK1 and VRK2 were never within the top 30% and were most often in the bottom 20% of kinases (Fig. 2F; Supplementary Fig. 2). Of note, another kinase that has been proposed to phosphorylate a number of sites on H3 including H3T3, PASK[70], was also not a notable hit in these screens (Fig. 2, Supplementary Fig. 2). Therefore, Haspin was reproducibly identified as the most likely mitotic H3T3 kinase in HeLa cell extracts.

A kinome-wide RNAi screen implicates Haspin, not VRKs, as the H3T3 kinase in mitosis. KiPIK screening uses cell extracts and appears to be relatively insensitive to the effects of upstream kinases in signaling cascades, and therefore is useful for identifying direct kinases for specific substrates[65]. As an alternative unbiased approach to screen for H3T3 kinases in a cellular environment, and in manner that would allow the possible indirect effect of kinases to be observed, we analysed the results of a kinome-wide RNAi screen for H3T3 kinases in mitotic HeLa cells[65]. Haspin was the top hit in this screen, and kinases known to regulate Haspin and the H3T3ph phosphatase Repo-Man-PP1 (i.e. Aurora B and Plk1[48–50,52]) were also present in the top 5 kinase hits (Fig. 3A). By contrast, none of the VRK kinases (nor PASK) were in the top 100 of the approximately 500 kinases tested. Therefore, RNAi screening also favours the hypothesis that Haspin, but not VRKs, are involved in the regulation of H3T3 in mitotic HeLa cells.

Targeted RNAi for VRK1 does not reveal a role in H3T3 phosphorylation. Although the RNAi screen uses multiple pre-validated siRNAs against each kinase, we could not be certain that VRK1 was depleted in these experiments. We therefore conducted targeted experiments to deplete VRK1 from HeLa cells by RNAi. We were able to reduce the amount of VRK1 by approximately 80% ± 10% (n = 5). In immunoblotting experiments, this did not detectably reduce the extent of H3T3ph in asynchronous cells or in cells arrested in mitosis with the microtubule destabilizing inhibitor nocodazole (Fig. 3B, Supplementary Table 1A). Immunofluorescence microscopy also confirmed that VRK1 depletion did not detectably alter H3T3ph in mitosis (Fig. 3C).

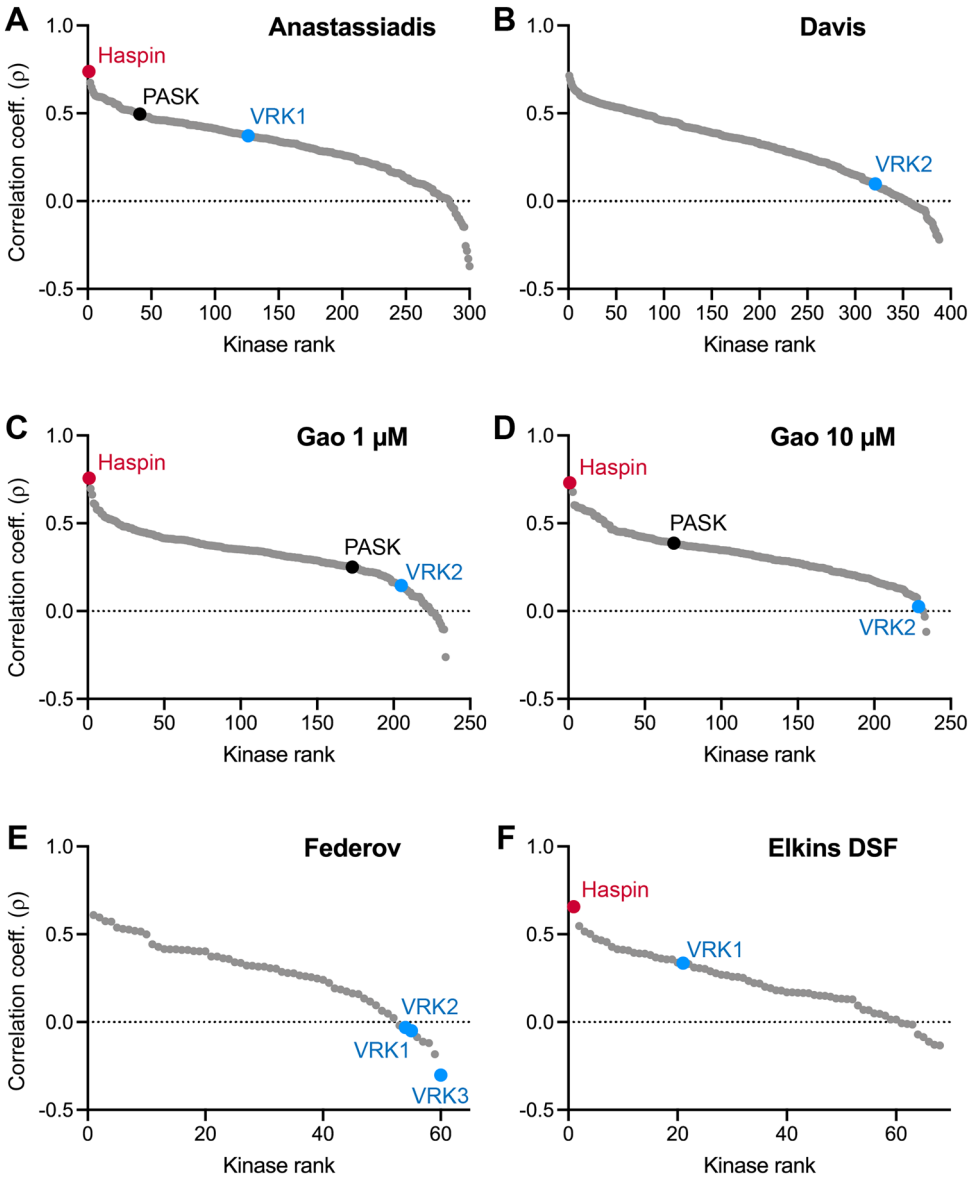

Figure 2. KiPIK screens for H3T3 kinase activity in mitotic HeLa cell lysates using the kinase profiling datasets of (**A**) Anastassiadis et al.[66], (**B**) Davis et al.[68], (**C**,**D**) Gao et al.[67], (**E**) Federov et al.[69] and (**F**) the differential scanning fluorimetry (DSF) method of Elkins et al.[99]. Some results of the Elkins DSF screen were previously published[65]. The ranking of Haspin (red), VRK1, VRK2, VRK3 (blue) and PASK (black) are shown for all datasets in which they appear.

By contrast, in HeLa cells lacking Haspin due to CRISPR/Cas9 targeting[14], H3T3ph could not be detected by immunoblotting or immunofluorescence microscopy (Fig. 3B,C). As expected[9,12,13], loss of Haspin did not alter the extent of H3S10ph in HeLa cells detected by immunoblotting (Fig. 3B, Supplementary Table 1A) or immunofluorescence (Fig. 3C). Consistent with this, loss of Haspin, but not VRK1, prevented detection of H3T3ph in mitotic cells containing H3S10ph (Fig. 3D). VRK1 depletion also did not cause a significant change in H3S10ph in immunoblotting experiments (Fig. 3B, Supplementary Table 1A), or in individual mitotic cells as determined by immunofluorescence microscopy (Fig. 3C), and progression through mitosis was not markedly altered in asynchronously growing cells (Supplementary Fig. 3). Therefore, using RNAi in HeLa cells, we could not uncover a role for VRK1 in phosphorylation of H3T3, or H3S10.

CRISPR/Cas9 targeting of VRK1 does not reveal a role in H3T3 phosphorylation. We were unable to remove all VRK1 from cells using RNAi, leaving open the possibility that low amounts of the kinase are able to maintain its putative role in H3 phosphorylation. To address this, we compared the effects of CRISPR/Cas9 targeting of Haspin and VRK1 in the haploid cell line HAP1 (see Supplementary Fig. 4). As expected, Haspin but not VRK1 could be detected in HAP1 VRK1 KO cells, and VRK1 but not Haspin could be seen in HAP1 Haspin KO cells (Fig. 4A). As in HeLa cells, loss of Haspin eliminated H3T3ph detectable by immunoblot-

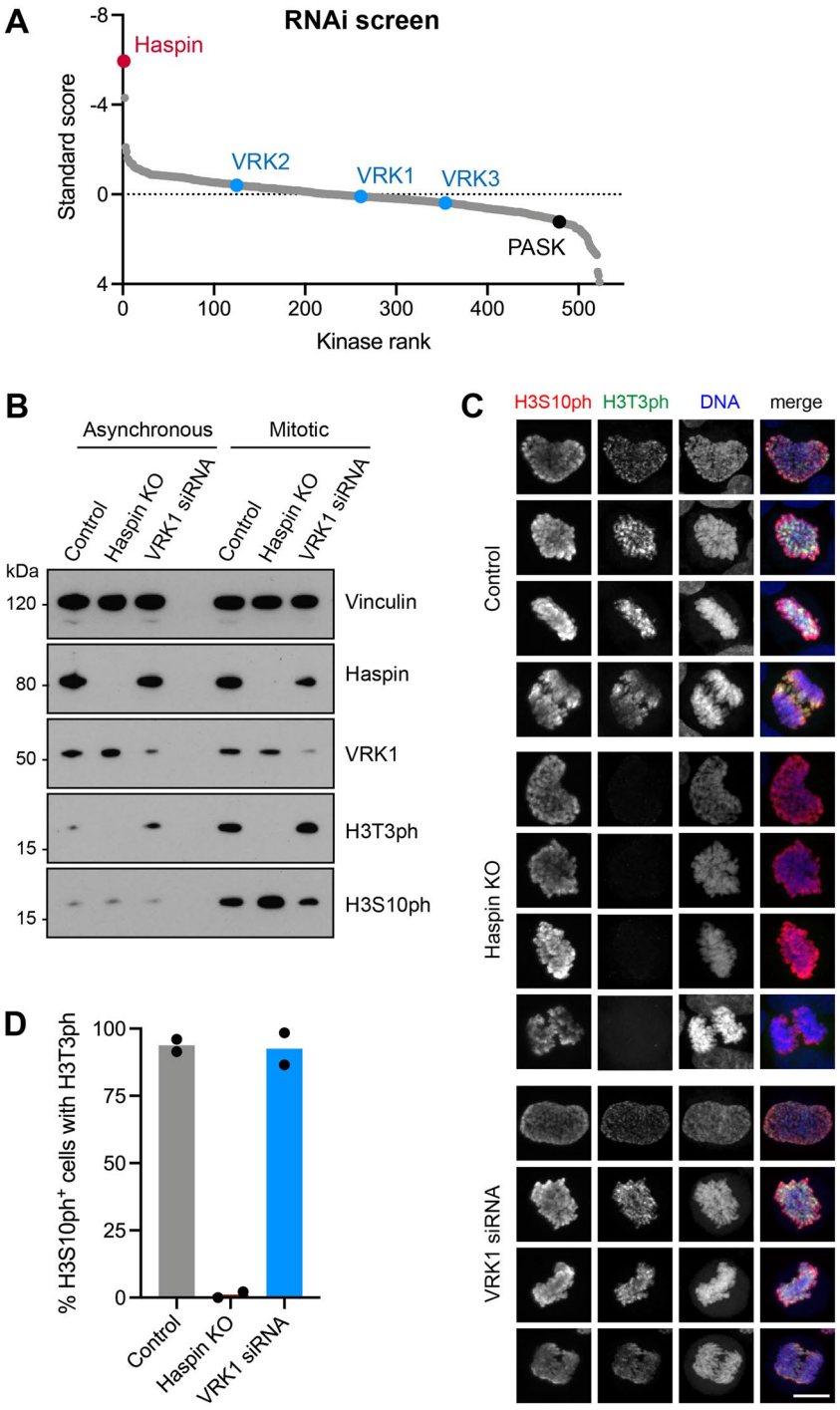

Figure 3. RNAi studies of VRK kinase function in mitosis. (**A**) Kinome-wide RNAi screen for kinases involved in H3T3 phosphorylation in HeLa cells. The standard score reflects the intensity of H3T3ph. Note that negative values indicate a decline in H3T3ph intensity. The ranking of Haspin (red), VRK1, VRK2, VRK3 (blue) and PASK (black) are shown. Some results of this screen were previously published[65]. (**B**) RNAi depletion of VRK1 from HeLa cells does not cause a significant loss of H3T3ph as detected by immunoblotting. The original blots are presented in Supplementary Fig. 7. (**C**) RNAi depletion of VRK1 does not cause a significant loss of H3T3ph or H3S10ph in individual mitotic HeLa cells, as detected by immunofluorescence microscopy. Scale bar, 10 µm. (**D**) Quantification of the proportion of HeLa cells in (**C**) with H3S10ph (i.e. mitotic cells) that also stain for H3T3ph.

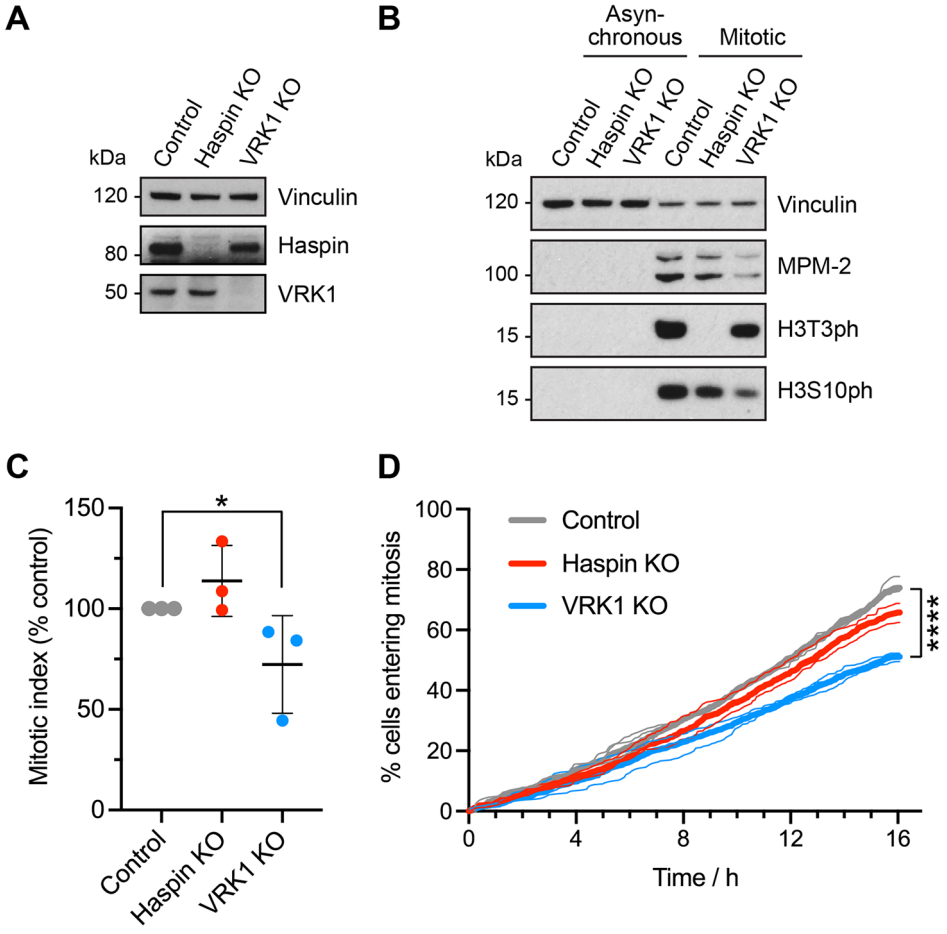

Figure 4. Histone H3 phosphorylation and cell division in control, Haspin KO and VRK1 KO HAP1 cells. (**A**) Immunoblotting shows the loss of Haspin in Haspin KO HAP1 cells, and the loss of VRK1 in HAP1 VRK1 KO cells. (**B**) Loss of VRK1 in HAP1 cells does not cause a significant loss of H3T3ph as detected by immunoblotting. The original blots are presented in Supplementary Fig. 7. (**C**) Control, Haspin KO and VRK1 KO HAP1 cells were allowed to accumulate in mitosis for 16 h in 300 nM nocodazole, and mitotic indices were then determined by immunofluorescence microscopy for MPM2. Error bars show means ± SD. *p = 0.045 (paired two-tailed Student *t* test using non-normalised data, n = 3). (**D**) Cumulative frequency of mitotic entry graphs for control, Haspin KO and VRK1 KO HAP1 cells observed by live imaging for 16 h. Between 193 and 555 cells were evaluated from three separate fields of view in each of three independent experiments, shown as thin lines. The combined results are shown as thick lines. Statistical significance was determined from the combined data using Kaplan–Meier curve analysis and a Mantel–Cox log rank test (****p < 0.0001). Mean cell cycle duration for Control, 24 h; Haspin KO, 26 h; and VRK1 KO, 33 h; 95% confidence intervals [23.5, 24.0], [26.0, 26.6] and [32.5, 33.0] respectively, as determined by linear regression.

ting of nocodazole-arrested mitotic HAP1 cells, but did not markedly affect H3S10ph (Fig. 4B; Supplementary Table 1B). By contrast, both H3T3ph and H3S10ph remained present in mitotic cells lacking VRK1 (Fig. 4B). The partial decline in both H3T3ph and H3S10ph often detected in mitotic cells by immunoblotting could be ascribed to the lower proportion of HAP1 VRK1 KO cells that accumulated in mitosis in nocodazole, as shown by the reduced intensity of Mitotic Protein Monoclonal-2 (MPM-2) phosphoepitopes seen by immunoblotting (Fig. 4B; Supplementary Table 1B), and by the lower mitotic index of nocodazole-treated HAP1 VRK1 KO cells compared to controls (Fig. 4C). Indeed, live imaging and cell counting revealed that, although the duration of mitosis was only slightly increased in HAP1 VRK1 KO cells (Supplementary Fig. 5A), they did proceed more slowly through interphase than HAP1 control or Haspin KO cells (Fig. 4D, Supplementary Fig. 5B), explaining why fewer VRK1 KO cells can accumulate in mitosis during exposure to nocodazole.

This interpretation was supported by quantifying the intensity of H3 phosphorylation in individual mitotic cells by immunofluorescence microscopy. Haspin KO HAP1 cells lost H3T3ph, but the intensity of H3T3ph in HAP1 VRK1 KO cells appeared unchanged throughout mitosis, and the intensity of H3S10ph appeared unaffected in both cell lines (Fig. 5, Supplementary Fig. 6A,B). Quantification of the number of cells with H3S10ph that also had H3T3ph confirmed this result (Supplementary Fig. 6C). These experiments also supported the view that progression through mitosis was minimally altered by loss of Haspin or VRK1 (Supplementary Fig. 6D).

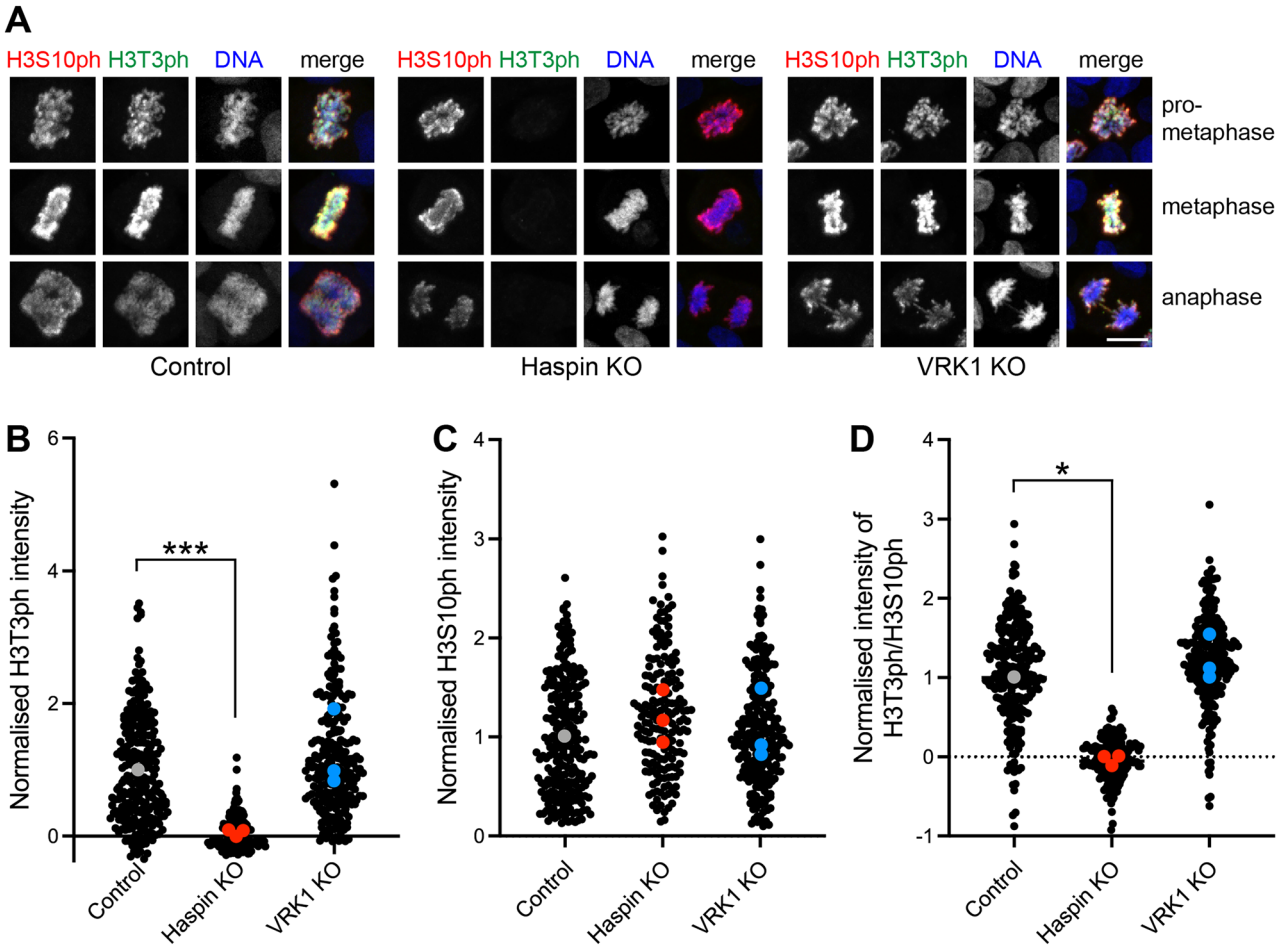

Figure 5. Immunofluorescence microscopy of histone H3 phosphorylation in HAP1 cells. (**A**) Loss of Haspin, but not VRK1, eliminates H3T3ph in individual mitotic HAP1 cells, as detected by immunofluorescence microscopy. H3S10ph appears unaffected in both cases. Scale bar, 10 µm. (**B**) Quantification of the intensity of H3T3ph staining in cells stained as in (**A**). Black symbols represent individual cells. Grey, red and blue symbols show the average values for each of 3 independent experiments, normalised to control HAP1 cells. ***p = 0.0019 (two-tailed *t* test using non-normalised data; n = 3). (**C**) Quantification of the intensity of H3S10ph staining in cells as in (**B**). Two-tailed *t* tests using non-normalised data revealed no significant differences at p = 0.05 (n = 3). (**D**) Quantification of the ratio of H3T3ph intensity to H3S10ph intensity in cells as in (**B**). *p = 0.0496 (two-tailed *t* test using non-normalised data; n = 3).

These results reveal that eliminating detectable VRK1 from HAP1 cells does not prevent normal H3T3 (or H3S10ph) phosphorylation in mitosis.

RNAi does not reveal a role for VRK2 in H3T3 phosphorylation. Human cells contain a second VRK1-related protein with kinase activity, VRK2. To determine if H3T3ph remaining in HAP1 VRK1 KO cells could be due to the presence of VRK2, we depleted VRK2 by RNAi. We were able to reduce VRK2 protein expression levels in the three HAP1 cell lines by 70 ± 13% (n = 9; Supplementary Table 1C). In immunoblotting experiments, this did not detectably reduce the extent of H3T3ph or H3S10ph in cells arrested in mitosis with the microtubule destabilizing inhibitor nocodazole (Fig. 6; Supplementary Table 1C). This was true even in VRK1 KO cells and in experiments where VRK2 depletion was most efficient, suggesting that VRK2 is not responsible for the persistence of H3T3ph in HAP1 VRK1 KO cells. As discussed earlier, HAP1 VRK1 KO cells had somewhat reduced levels of H3S10ph and MPM2 phosphoepitopes detected by immunoblotting (Supplementary Table 1C), most likely explained by the decline in the proportion of mitotic cells.

Discussion

Here, in vitro, we find that Haspin is a much more potent kinase than VRK1 for H3T3 and that VRK1 phosphorylates BAF much more strongly than the multiple potential phosphorylation sites on recombinant H3. Interestingly, the only VRK1 preparation that was able to phosphorylate H3 significantly was GST-VRK1 isolated from *E. coli*, and this ability was lost when the GST tag was removed. Notably, previous studies reporting phosphorylation of H3 by purified recombinant VRK1 in vitro have used GST-VRK1[19–23,47]. The reason for this effect of the GST tag remains to be determined, but it could be that GST alters the conformation or affinity of VRK1 in a

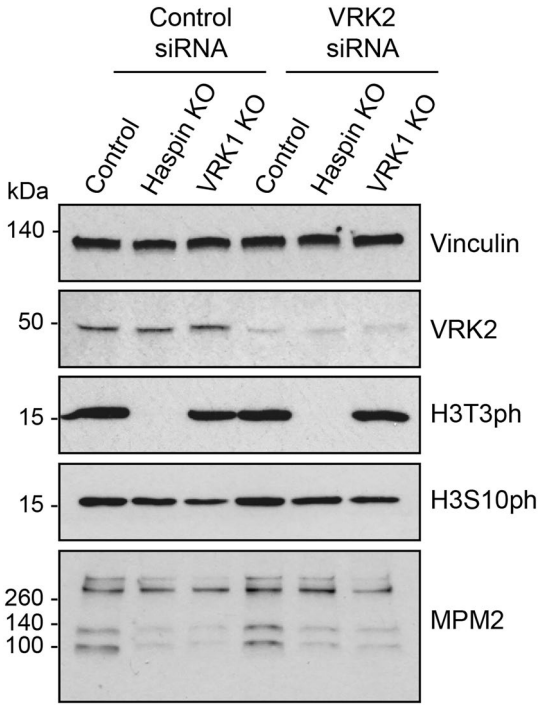

Figure 6. RNAi of VRK2 does not have a detectable influence on H3T3ph. Control and VRK1 KO HAP1 cells were treated with control or VRK2 siRNAs and subjected to immunoblotting with the stated antibodies. Note that the top 3 panels are from a different immunoblot from the one in the bottom 2 panels. The original blots are presented in Supplementary Fig. 7.

way that enables it to phosphorylate H3, or that GST leads to the co-purification of a contaminating protein that enables H3 phosphorylation. A recent report that untagged VRK1 can phosphorylate nucleosomal H3T3 in vitro only when the nucleosomes contain additional linker DNA is interesting, but it is possible that the linker DNA enhances non-specific interaction of VRK1 with nucleosomes, and the activity appeared weak compared to that of VRK1 towards BAF[25]. These will be important considerations for future in vitro studies of VRK1.

In addition, using KiPIK assays in mitotic HeLa cell extracts, none of the VRK family kinases are found to be strong candidates for the H3T3 kinase in mitosis while, in contrast, Haspin was the highest ranked kinase. Similarly, in a kinome-wide RNAi screen for mitotic H3T3ph kinases, Haspin was the top hit, while none of the VRKs were in the top 100. CRISPR/Cas9 targeting of Haspin, but not VRK1, caused loss of detectable H3T3ph during mitosis in HAP1 cells. Furthermore, depleting VRK2 in combination with loss of VRK1 did not lead to detectable reductions in H3T3ph, suggesting that redundancy with VRK2 does not underlie our failure to influence H3T3ph when VRK1 expression is ablated. VRK3 is unlikely to contribute as it is a pseudokinase with a degraded active site structure[31] that is unable to bind divalent cations or ATP[71], and is unable to phosphorylate casein or H3[20,72]. In addition, PASK did not score highly as a mitotic H3T3 kinase in either KiPIK or RNAi screens, concordant with the finding that CRISPR/Cas9 targeting of the PASK gene did not markedly alter H3T3ph in mouse C2C12 cells[70]. Our study also illustrates how KiPIK assays[65] provide a new and rapid way to examine which kinase is predominantly responsible for directly phosphorylating specific substrate sites in defined biological contexts.

These results suggest that Haspin is the major H3T3 kinase during mitosis in human cells. This is consistent with reports that Haspin is required for normal mitotic H3T3ph in mouse cells[3], sea urchin embryos[73], fruit flies[74,75], *Arabidopsis*[76,77], and fission yeast[6], and for H3T3ph during meiosis in mouse oocytes[78,79] and frog egg extracts[5]. Indeed, Haspin orthologues are present in all organisms that are reported to have H3T3ph in mitosis to date. By contrast, VRK family kinases are present in many metazoa (e.g., VRK-1 in *C. elegans*, and NHK-1/ballchen in *Drosophila*) but appear absent from plants and yeasts[28,72].

It remains uncertain why previous experiments have suggested a role for VRK1 in producing H3T3ph in mitosis. However, multiple reports indicate that VRK1 influences cell cycle progression. VRK1 regulates the expression of Cyclin D1, and VRK1 depletion impedes progression from G1 to S phase in cultured human cells[35,80–83]. This could hinder cells reaching mitosis and so lead to a loss of modifications that are abundant during this time, such as H3T3ph and H3S10ph. Indeed, although it is clear that HAP1 cells lacking detectable VRK1 can proliferate in culture, live imaging revealed that a lower proportion of VRK1 KO cells enter mitosis per unit time, consistent with a delay in the cell cycle outside mitosis, such as during G1. In addition, a previous report found that a high proportion of HeLa cells die in mitosis following VRK1 RNAi[64]. The loss of H3 phosphorylation seen in previous immunoblotting experiments that used nocodazole to accumulate mitotic cells, therefore, may be an indirect effect of a reduced mitotic index. By contrast, in experiments where the intensities of H3T3ph and H3S10ph in individual mitotic cells were measured, we found no evidence for a decline in these phosphorylation marks.

Analysis of VRK1 function in cell division in model organisms is complicated because complete loss of function is lethal in mice, flies and worms[34,61,84], so only hypomorphic alleles or the results of partial depletions have been examined. Male and female VRK1$^{GT3/GT3}$ gene-trapped mice are infertile, indicating defects in gametogenesis. Indeed, there is a strong defect in proliferation of spermatogonial cells in male mice, commensurate with their reduced levels of cell cycle markers such as Proliferating Cell Nuclear Antigen (PCNA). The reduction in H3S10ph in these testes is most likely due to the reduced numbers of proliferating cells, not a specific loss of H3S10ph due to reduced VRK1 function[32]. Consistent with this, the infertility of female VRK1$^{GT3/GT3}$ mice appears to be due to meiotic defects in oocytes, but these oocytes have normal levels of H3S10ph[85].

Hypomorphic NHK-1 mutant female flies are also infertile, and have defects in clustering and condensation of chromosomes in oocytes[84,86]. Mitotic chromosome condensation and segregation are abnormal in NHK-1-depleted *Drosophila* S2 cells and in NHK-1 mutant fly larvae, as well as in VRK-1-depleted *C. elegans* embryos[61,63,84]. Notably, increases in the number of mitotic cells are common in hypomorphic NHK-1 mutant fly embryos and larvae, consistent with prolonged mitosis. In contrast, the proportion of mitotic cells *decreases* in embryos with lethal NHK-1 mutations[63,84,86], suggesting cell cycle defects prior to mitosis. However, in both cases, H3S10ph levels appear normal in individual mitotic cells, arguing against a direct role for NHK-1 in phosphorylating H3S10[63]. Similar results were obtained in cultured human cells arrested in mitosis, where VRK1 RNAi did not influence H3S10ph[62].

Putting together these findings, the reason that alterations in VRK1 activity give rise to different cell cycle defects in different systems may be due to the different mutants analysed and varying degrees of depletion obtained in different experiments. In addition, the extent to which other kinases such as VRK2 can act redundantly may vary depending on the organism, cell type, or function in question[41,58]. Indeed, there is a second VRK-related kinase in *Drosophila*, CG8878, although it has a distinctive split kinase domain and its molecular function remains unclear[87]. Nevertheless, there is strong evidence that VRK1 deficiency affects both mitosis and meiosis. However, our results suggest these effects are unlikely to be due to changes in H3T3ph phosphorylation. While we cannot fully exclude the possibility that VRKs are involved in H3T3 phosphorylation in other cell types, we find no strong evidence for a role in vitro, nor in two distinct cell lines, including the HeLa cells used in the original study[19] (derived from a cervical epithelial cancer), and HAP1 (derived from chronic myelogenous leukemia cells). In addition, H3S10ph does not appear to be directly affected by loss of VRK1, in line with other studies discussed above[32,62,63,83]. Interestingly, fly NHK-1 and human VRK1 have also been reported to phosphorylate nucleosomal H2AT120 (H2AT119 in flies)[59,82]. Phosphorylation of this site is clearly elevated in mitosis and meiosis in human cells, flies, budding and fission yeast[18,59,86,88]. An NHK-1 mutation that causes infertility in female flies diminishes H2AT119ph in oocytes[86], but whether this is a direct or indirect effect of NHK-1 on H2A phosphorylation remains unknown. Oocytes of VRK1$^{GT3/GT3}$ mice have normal levels of H2AT120ph[85]. Moreover, neither mutation nor depletion of NHK-1 prevents mitotic H2AT119ph in flies or *Drosophila* S2 cells[86,88]. Instead, the kinetochore-binding kinase Bub1 is clearly vital for H2AT120ph in budding and fission yeast, mice, and human cells[18,89,90]. Together, there is little evidence to support a significant role for VRK1 in direct phosphorylation of H3T3ph or other histone residues in mitosis.

VRK1 phosphorylates and inhibits Barrier-to-Autointegration Factor (BAF) to regulate nuclear envelope dissolution during mitosis and meiosis in flies, worms and mammalian cells[41,45,58,60–64], and this seems likely be a major contributor to its cell division phenotypes. In addition, we have not ruled out a role for VRK1 in histone phosphorylation outside mitosis. Worm VRK-1 is expressed in post-mitotic cells and can influence lifespan by activating AMP-activated protein kinase[91], and Aihara et al. have suggested that VRK1 regulates gene expression by phosphorylating H2AT120 at gene promoters such as *CCND1*/Cyclin D1 in mice[82]. A number of H3S10 kinases that act to regulate transcription in interphase cells have been characterized, including MSK1/2[28,33]. It is possible that Haspin itself has functions outside mitosis[75,92], and the plant-specific MUT9 kinases generate H3T3ph in *Chlamydomonas* and *Arabidopsis* and appear to be involved in epigenetic silencing[93,94]. Interestingly, like the VRK family, MUT9 kinases are part of the CK1 superfamily and it is conceivable that VRKs serve a similar function in metazoa. It also will be interesting in future to determine if the mitotic or non-mitotic functions of VRK1 underlie the neuromuscular disorders observed in mice and human patients[30,55–57].

Methods

Cell culture and transfection. HeLa cells, HeLa clone D2 Haspin KO cells[14], and parental controls, were maintained in DMEM with 10% (v/v) FBS, 100 U/ml penicillin and streptomycin and 2 mM L-glutamine at 37 °C and 5% CO_2 in a humidified incubator. HAP1 knock out cell lines for GSG2 (Haspin; HZGHC000047c016) and VRK1 (HZGHC000073c014), as well as a parental control line (C631), were obtained from Horizon Discovery (Cambridge, UK) and maintained in IMDM with 10% (v/v) FBS, 100 U/ml penicillin and streptomycin and 2 mM L-glutamine at 37 °C and 5% CO_2 in a humidified incubator. HeLa D2 parental control cells were transfected with 300 ng/ml human VRK1 MISSION® esiRNA (EHU119541, Sigma) using HiPerFect Transfection Reagent (301707, Qiagen) and analysed after 24 h. HAP1 cells were transfected with 600 ng/ml human VRK2 MISSION® esiRNA (EHU070731, Sigma-Aldrich) using Lipofectamine RNAiMAX (13778075, ThermoFisher) and analysed after 24 h. MISSION® siRNA Universal Negative Control (SIC001, Sigma-Aldrich) was used at an equal concentration as the control for RNAi experiments. Where stated, cells were blocked in mitosis by treatment with 300 nM nocodazole (Sigma) for 16 h.

Cell counting. HAP1 cell lines were counted using trypan blue (Sigma) and a haemocytometer, seeded at 100,000 cells/well in 6-well plates, and recounted at 24 h intervals.

SDS-PAGE and immunoblotting. Cells were washed once in PBS and then lysed in 141 mM Tris Base, 106 mM Tris HCl, 2% LDS, 1% Benzonase nuclease (E1014, Millipore), pH 8.5, at room temperature for 15 min and snap frozen in liquid nitrogen. The protein concentration was determined using Rapid Gold BCA Protein Assay Kit (Pierce). Cell lysates (20 µg) were run on NuPAGE 4–12% Bis–Tris protein gels (Invitrogen) using standard procedures, transferred to 0.2 µm polyvinylidene fluoride membranes and blocked in 5% milk in TBST (0.05% Tween 20 in Tris-buffered saline) for 1 h at room temperature before overnight incubation with primary antibodies. Membranes were washed thrice in TBST then incubated with a HRP conjugated secondary antibody for 1 h at room temperature in TBST with 5% milk, and signals were detected by chemiluminescence (Clarity ECL, Biorad). Antibodies used in immunoblotting were as follows: rabbit polyclonal anti-Vinculin (Cell Signaling Technology, #13901), anti-Haspin (Abcam, ab21686, lot 156753), and anti-H3T3ph (B8634[9]) with anti-rabbit IgG HRP (Cell Signaling Technology, #7074) and mouse monoclonal anti-VRK1 (Abcam, ab171933), anti-VRK2 (Santa Cruz, sc-365199), anti-H3S10ph (Millipore, 05-806), anti-α-tubulin (B-5-1-2, Sigma, T5168) and anti-MPM2 (Millipore, 05-368) with anti-mouse IgG HRP (Cell Signaling Technology, #7076).

Immunofluorescence. Cells were fixed for 10 min with 4% paraformaldehyde in PBS, washed twice in PBS, then permeabilized for 5 min with 0.5% Triton X-100 in PBS. After washing twice in PBS, cells were incubated for 1 h in 5% BSA in PBS, 0.05% Tween20 at room temperature, and then with primary rabbit antibody against H3T3ph (B8634) and, in some cases, with mouse anti-MPM2, at 37 °C in 5% BSA in PBS, 0.5% Tween20. After washing twice with 0.05% Tween20 in PBS, cells were incubated for 1 h with fluorophore-conjugated secondary antibody anti-rabbit-IgG Alexa Fluor®488 (Invitrogen A32731) and, where necessary, anti-mouse IgG-Alexa Fluor®594 (Invitrogen, A-32744) at 37 °C in 5% BSA in PBS, 0.5% Tween20. After washing twice with PBS, 0.5% Tween20, cells were incubated with rabbit phospho-Histone H3 (Ser10) (D2C8) XP® mAb directly conjugated to Alexa Fluor®647 (Cell Signaling Technology, #3458) for 1 h at room temperature. After washing twice with PBS, 0.5% Tween20, and once with milliQ H_2O, samples were mounted using ProLong™ Diamond Antifade Mountant with DAPI (ThermoFisher, P36962). Images were captured on a Nikon A1 confocal microscope with a 20 × Air/NA 0.75 or 60 × Oil/NA 1.4 objectives using Nikon Elements software.

Quantification of immunofluorescence. To quantify immunofluorescence intensities in individual cells, and to determine mitotic indices, images were analysed in Fiji 2.0[95]. Cells were identified from DAPI staining by automatic thresholding of maximum intensity projections and binarization followed by use of the watershed tool to separate adjacent cells. Cells were then counted using the analyse particles tool with a minimum cut off of 20 μm^2. The fluorescence intensities for H3T3ph and H3S10ph in each cell were quantified using sum intensity projections. Cells in mitosis were identified as those whose fluorescence intensity for H3S10ph classified them as outliers from the majority of interphase cells using the iterative Grubbs' method ($\alpha = 0.0001$) in Prism 9.0.2 (GraphPad). Visual inspection of DAPI stained cells confirmed that, for H3S10ph, this included essentially all mitotic cells. Automatically identified particles containing more than one mitotic cell were eliminated from the analysis. Background fluorescence was determined from the average fluorescence intensity of all non-mitotic cells, and values were standardised such that the mean intensity of all control mitotic cells was equal to 1. MPM2 positive cells were identified similarly with the additional use of the fill holes tool prior to watershedding.

Live imaging. Live imaging was performed in glass-bottomed FluoroDishes (WPI) in IMDM medium (12440053, ThermoFisher). DNA was stained with 25 nM SiR-DNA (Spirochrome). DIC and SiR-DNA images at 6 z-steps per field (2 µm step size) were acquired at 4 min intervals on a Nikon A1R confocal microscope equipped with a 20 × 0.75 NA PlanApo VC DIC objective using Elements v5.22 software (Nikon, Japan). In a blinded fashion, the time of mitotic entry was determined as the earliest time point at which the initiation of cell rounding was observed by DIC and/or the time point prior to nuclear envelope breakdown observed by SiR-DNA staining, and the time of mitotic exit was defined as the first frame in which anaphase was apparent.

KIPIK screens. To prepare mitotic cell extract, HeLa cells were treated with 300 nM nocodazole for 15 h, collected by shake off , and lysed at 4 °C in 50 mM Tris, 0.25 M NaCl, 0.1% Triton X100, 10 mM $MgCl_2$, 2 mM EDTA, 1 mM DTT, pH 7.5 with protease inhibitor cocktail (Sigma P8340), PhosSTOP (Merck), 1 mM PMSF, 0.1 µM okadaic acid, 10 mM NaF, 20 mM β-glycerophosphate, at approximately 30×10^6 cells/ml. Extracts were immediately flash frozen in liquid nitrogen. Kinase reactions contained 10 µM kinase inhibitor or DMSO (vehicle control), 0.35 µM Histone H3(1–21) peptide (ARTKQTARKSTGGKAPRKQLA-GGK-biotin; Abgent), 0.2 mM ATP and 5% cell extract, in KiPIK buffer [50 mM Tris, 10 mM $MgCl_2$, 1 mM EGTA, 10 mM NaF, 20 mM β-glycerophosphate, 1 mM PMSF, pH 7.5 with PhosSTOP (Merck)]. Reactions were carried out in duplicate in 384-well microplates (ThermoFisher), at 37 °C for 30 min, in a total volume of 35 µl/well. An expanded custom library of inhibitors similar to that described previously[65] was used (Supplementary Data 1).

For detection of phosphorylation, High Capacity Streptavidin-coated 384-well plates (Pierce) were washed thrice with TBS, 0.1% Tween20, then, 35 µl/well of completed KiPIK extract kinase reaction were added and incubated at room temperature for 1 h. After washing, 0.2 µg/ml H3T3ph B8634 antibodies were added at 40 µl/well in TBS, 0.1% Tween20, 5% BSA, for 1 h at room temperature. After washing, 40 µl/well of HRP-conjugated anti-rabbit IgG antibodies (Cell Signaling Technology, #7074) in TBS, 0.1% Tween20, 5% BSA were added for 1 h at room temperature. After washing, HRP-conjugated antibody binding was detected using TMB substrate (New England Biolabs) according to the manufacturer's instructions. Pipetting was performed with a Biomek FX liquid handling robot (Beckman Coulter). Absorbance readings were made using a Polarstar Omega microplate reader (BMG Labtech).

KIPIK results analysis. Using the mean of duplicate determinations, a standard score reflecting kinase activity in the presence of each inhibitor was calculated where standard score = (mean absorbance in presence of inhibitor – mean absorbance of multiple DMSO controls)/standard deviation of DMSO controls. The inhibition by each compound was defined as: %inhibition = 100 × (standard score for inhibitor/lowest standard score on plate). The %inhibition scores for all inhibitors were then compiled to produce the inhibition fingerprint of H3T3 phosphorylation. Using Excel (Microsoft), Pearson's correlation (ρ) was then calculated for this fingerprint against the inhibition profiles of each of the kinases profiled in vitro against that inhibitor library, excluding mutant kinases. We calculated z-scores where z = (observed ρ – mean ρ of null distribution)/standard deviation of null distribution as described[65].

Recombinant VRK1. Human VRK1 carrying an N-terminal 3xFLAG tag was produced in lentivirally-transduced stable human MCF10A cells[96]. Cells were lysed in FLAG lysis buffer (20 mM Tris, 150 mM NaCl, 1% Triton X-100, 2 mM $MgCl_2$, pH 7.4) with 25 U/ml Benzonase (Novagen) and protease inhibitors at 4 °C for 15 min. After centrifugation, nuclear material was resuspended in FLAG lysis buffer with 500 mM NaCl for 30 min at 4 °C, combined with the cytoplasmic supernatant, and incubated with FLAG M2 antibody resin (Sigma-Aldrich) for 3 h at 4 °C. After washing in 20 mM Tris, 150 mM NaCl, pH 7.4, the 3xFLAG-VRK1 was eluted by the addition of 3 × FLAG peptide (Sigma). Eluted 3xFLAG-VRK1 was supplemented with 5 mM EDTA, 5 mM DTT, and 15% glycerol.

Human VRK1 with an N-terminal His tag was purified from *E. coli* HMS174 containing pET16b-VRK1[72] induced with 1 mM IPTG and infection with λCE6 encoding T7 RNA polymerase. Bacteria were resuspended in 5 mg/ml lysozyme in lysis buffer (20 mM Tris, 500 mM NaCl, 0.1% Triton X-100, 10 mM imidazole, pH 8) with protease inhibitors for 30 min at 4 °C, followed by 3 rounds of freeze-thawing, and then sonication. Clarified lysates were incubated with Ni-NTA agarose (Thermo Scientific) for 2 h at 4 °C, and then the resin was washed sequentially with lysis buffer, lysis buffer with 50 mM imidazole, and lysis buffer with 70 mM imidazole. His-VRK1 was eluted with lysis buffer supplemented with 0.25 M imidazole, and dialyzed into 25 mM Tris, 100 mM NaCl, 1 mM EDTA, and 10% glycerol, pH 8.

GST tagged human VRK1 was produced from IPTG-induced *E. coli* BL21 carrying pGEX-6P-1-VRK1. Bacteria were sonicated in PBS (140 mM NaCl, 2 mM KCl, 10 mM Na_2PO_4, 1 mM KH_2PO_4) supplemented with protease inhibitors, with the subsequent addition of 1% Triton X-100. The soluble fraction was incubated with glutathione Sepharose 4B beads (GE Healthcare) in PBS at 4 °C, the resin washed with PBS 3 times, and then GST-VRK1 eluted with 50 mM Tris HCl, 20 mM reduced glutathione, pH 8, and dialysed into 50 mM Tris, 150 mM NaCl, 1 mM EDTA, 1 mM DTT, and 10% glycerol, pH 7.4.

To prepare untagged human VRK1, GST-VRK1 was cleaved with PreScission protease (GE Healthcare) at 4 °C for 22 h, and glutathione-Sepharose was used to remove free GST and the GST-tagged PreScission protease.

Recombinant BAF and anti-BAF S4ph. Recombinant wild type human BAF dimers were purified from IPTG-induced *E. coli* BL21(DE3)pLysS carrying pET-15b-BAF essentially as described[45,97]. Briefly, after sonication in 25 mM Tris, 150 mM NaCl, 5 mM imidazole, 5% glycerol, 0.01% lysozyme, pH 7.4, and centrifugation, the pellet was suspended in denaturing buffer (25 mM Tris, 150 mM NaCl, 5 mM imidazole, 6 M guanidine hydrochloride, 5% glycerol, pH 7.4) for 10 min. After re-centrifugation, His-BAF was purified from the soluble fraction using Ni-NTA beads, washed once with 25 mM Tris, 1.5 M guanidine hydrochloride, 150 mM NaCl, 25 mM imidazole, 5% glycerol, pH 7.4, twice in the same buffer with 50 mM imidazole, and once more with the same buffer with 75 mM imidazole. His-BAF was eluted in the same buffer containing 0.3–0.5 M imidazole, and then refolded by dialysis into 100 mM K_2HPO_4, 200 mM NaCl, 5% glycerol, 10 mM EDTA, and 10 mM 2-mercaptoethanol, pH 6.5. After concentration, the His tag was cleaved using thrombin for 3 h at 25 °C. Thrombin was removed using a benzamidine-Sepharose column (Amersham). Finally, gel exclusion chromatography was performed in 20 mM Tris, 150 mM NaCl, 0.1 mM EDTA, 10 mM DTT, and 10% glycerol, pH 7.4, using a Sephacryl S100 10/80 column (Amersham).

Recombinant human BAF in which all 4 cysteines are mutated into alanine, was produced from a codon-optimised cDNA with a His-tag[98] in *E. coli* BL21 DE3 Star. After sonication in 50 mM Tris, 300 mM NaCl, 5% glycerol, 0.1% Triton X-100, pH 8, and centrifugation, the pellet was suspended in purification buffer (50 mM Tris, 150 mM NaCl, 8 M urea, pH 8) for 20 min. After re-centrifugation, His-BAF was purified from the soluble fraction using Ni-NTA beads, washed with purification buffer, and eluted in the same buffer supplemented with 1 M imidazole. His-BAF was then refolded by dialysis into 50 mM Tris, 150 mM NaCl, pH 8. After concentration, the His tag was cleaved using His-tagged TEV protease overnight at 4 °C. The cleaved His-tag and His-tagged TEV protease were then removed using Ni-NTA beads. The resulting BAF protein (which, after cleavage, has glycine instead of methionine at position 1) was collected in the flow-through. Finally, gel exclusion chromatography was performed in 50 mM HEPES, 150 mM NaCl, pH 7.4, using a Superdex 200 pg HiLoad 10/600 column (Cytiva).

Rabbit antibodies to BAF phosphorylated at Ser-4 (BAF S4ph) were generated using the KLH-conjugated BAF(1–10) peptide MTT-S4ph-QKHRDFC (YenZym Antibodies LLC). Phosphospecific antibody was then isolated from serum by sequential positive and negative affinity purification. The antibody recognised a BAF(1–16) S4ph peptide (MTT-S4ph-QKHRDFVAEPMGK-biotin; Eurogentec) in preference to the unphosphorylated BAF(1–16) peptide (MTTSQKHRDFVAEPMGK-biotin; Eurogentec) in an ELISA carried out as described for KiPIK detection above (Supplementary Fig. 1A).

In vitro kinase assays. When using antibody-based detection, in vitro kinase reactions contained the stated kinase concentrations, 0.35 μM H3(1–21)-GGK-biotin peptide (Abgent), 0.35 μM recombinant bioti-

nylated human mononucleosomes (16-0006, Epicypher), or 0.1 µM recombinant human BAF, and 0.2 mM ATP in KiPIK buffer. Reactions were carried out in triplicate in 384-well microplates (ThermoFisher), at 37 °C for 30 min, in a total volume of 35 µl/well. The kinases used were: full-length GST-VRK1 produced in *E. coli* (P5776, Abnova), FLAG-VRK1 produced in *E. coli* (31243, Active Motif), GST-VRK1 produced in insect Sf9 cells (ab125555, Abcam) and 6His-Haspin residues 471–798 produced in *E. coli*[9]. Phosphorylation was detected as described for KiPIK experiments above or, for BAF, using a sandwich ELISA in microplates coated with 4 µg/ml mouse monoclonal anti-BAF (sc-166324 X, Santa Cruz), and 0.8 µg/ml rabbit anti-BAF S4ph as the detection antibody.

For [γ^{32}P]-ATP incorporation assays, recombinant 3xFLAG-VRK1, His-VRK1, GST-VRK1, or untagged VRK1 (produced as described in the section "Recombinant VRK1") were incubated with recombinant Histone H3 (14–494, Millipore) or BAF at the stated concentrations in 50 mM Tris, 5 mM $MgCl_2$, 0.5 mM DTT, 150 mM KCl, 10 µM ATP, 5 µCi [γ^{32}P] ATP, pH 7.5 at 25 °C for 60 min. Reactions were stopped by addition of SDS-PAGE sample buffer, analysed by SDS-PAGE, and visualised by phosphorimaging.

Statistical analysis. Statistical analyses were carried out using Prism 9.0.2 (Graphpad).

Data availability

Data generated and analysed during this study are included in this published article (and its Supplementary Information files). Additional data are available from the corresponding author on reasonable request.

Received: 7 February 2022; Accepted: 22 June 2022
Published online: 01 July 2022

References

1. Wang, F. & Higgins, J. M. G. Histone modifications and mitosis: Countermarks, landmarks, and bookmarks. *Trends Cell Biol.* **23**, 175–184 (2013).
2. Polioudaki, H. *et al.* Mitotic phosphorylation of histone H3 at threonine 3. *FEBS Lett.* **560**, 39–44 (2004).
3. Dai, J. & Higgins, J. M. G. Haspin: A mitotic histone kinase required for metaphase chromosome alignment. *Cell Cycle* **4**, 665–668 (2005).
4. Wang, F. *et al.* Histone H3 Thr-3 phosphorylation by Haspin positions Aurora B at centromeres in mitosis. *Science* **330**, 231–235 (2010).
5. Kelly, A. E. *et al.* Survivin reads phosphorylated histone H3 threonine 3 to activate the mitotic kinase Aurora B. *Science* **330**, 235–239 (2010).
6. Yamagishi, Y., Honda, T., Tanno, Y. & Watanabe, Y. Two histone marks establish the inner centromere and chromosome bi-orientation. *Science* **330**, 239–243 (2010).
7. Carmena, M., Wheelock, M., Funabiki, H. & Earnshaw, W. C. The chromosomal passenger complex (CPC): From easy rider to the godfather of mitosis. *Nat. Rev. Mol. Cell Biol.* **13**, 789–803 (2012).
8. Varier, R. A. *et al.* A phospho/methyl switch at histone H3 regulates TFIID association with mitotic chromosomes. *EMBO J.* **29**, 3967–3978 (2010).
9. Dai, J., Sultan, S., Taylor, S. S. & Higgins, J. M. G. The kinase haspin is required for mitotic histone H3 Thr 3 phosphorylation and normal metaphase chromosome alignment. *Genes Dev.* **19**, 472–488 (2005).
10. Eswaran, J. *et al.* Structure and functional characterization of the atypical human kinase haspin. *Proc. Natl. Acad. Sci. U.S.A.* **106**, 20198–20203 (2009).
11. Markaki, Y., Christogianni, A., Politou, A. S. & Georgatos, S. D. Phosphorylation of histone H3 at Thr3 is part of a combinatorial pattern that marks and configures mitotic chromatin. *J. Cell Sci.* **122**, 2809–2819 (2009).
12. Wang, F. *et al.* Haspin inhibitors reveal centromeric functions of Aurora B in chromosome segregation. *J. Cell Biol.* **199**, 251–268 (2012).
13. De Antoni, A., Maffini, S., Knapp, S., Musacchio, A. & Santaguida, S. A small-molecule inhibitor of Haspin alters the kinetochore functions of Aurora B. *J. Cell Biol.* **199**, 269–284 (2012).
14. Zhou, L. *et al.* The N-terminal non-kinase-domain-mediated binding of haspin to Pds5B protects centromeric cohesion in mitosis. *Curr. Biol.* **27**, 992–1004 (2017).
15. Dai, J., Sullivan, B. A. & Higgins, J. M. G. Regulation of mitotic chromosome cohesion by Haspin and Aurora B. *Dev. Cell* **11**, 741–750 (2006).
16. Liang, C. *et al.* Centromere-localized Aurora B kinase is required for the fidelity of chromosome segregation. *J. Cell Biol.* **219**, e201907092 (2020).
17. Hadders, M. A. *et al.* Untangling the contribution of Haspin and Bub1 to Aurora B function during mitosis. *J. Cell Biol.* **219**, e201907087 (2020).
18. Kawashima, S. A., Yamagishi, Y., Honda, T., Ishiguro, K. & Watanabe, Y. Phosphorylation of H2A by Bub1 prevents chromosomal instability through localizing shugoshin. *Science* **327**, 172–177 (2010).
19. Kang, T. H. *et al.* Mitotic histone H3 phosphorylation by vaccinia-related kinase 1 in mammalian cells. *Mol. Cell. Biol.* **27**, 8533–8546 (2007).
20. Sanz-Garcia, M., Lopez-Sanchez, I. & Lazo, P. A. Proteomics identification of nuclear Ran GTPase as an inhibitor of human VRK1 and VRK2 (vaccinia-related kinase) activities. *Mol. Cell. Proteomics* **7**, 2199–2214 (2008).
21. Jeong, M. W., Kang, T. H., Kim, W., Choi, Y. H. & Kim, K. T. Mitogen-activated protein kinase phosphatase 2 regulates histone H3 phosphorylation via interaction with vaccinia-related kinase 1. *Mol. Biol. Cell* **24**, 373–384 (2013).
22. Salzano, M., Sanz-Garcia, M., Monsalve, D. M., Moura, D. S. & Lazo, P. A. VRK1 chromatin kinase phosphorylates H2AX and is required for foci formation induced by DNA damage. *Epigenetics* **10**, 373–383 (2015).
23. Moura, D. S., Campillo-Marcos, I., Vazquez-Cedeira, M. & Lazo, P. A. VRK1 and AURKB form a complex that cross inhibit their kinase activity and the phosphorylation of histone H3 in the progression of mitosis. *Cell. Mol. Life Sci.* **75**, 2591–2611 (2018).
24. Fehri, L. F. *et al.* Helicobacter pylori-induced modification of the histone H3 phosphorylation status in gastric epithelial cells reflects its impact on cell cycle regulation. *Epigenetics* **4**, 577–586 (2009).
25. Budziszewski, G. R. *et al.* Multivalent DNA and nucleosome acidic patch interactions specify VRK1 mitotic localization and activity. *Nucleic Acids Res.* **50**, 4355–4371 (2022).
26. Kim, W. *et al.* Macro histone H2A1.2 (macroH2A1) protein suppresses mitotic kinase VRK1 during interphase. *J. Biol. Chem.* **287**, 5278–5289 (2012).

27. Valbuena, A., Lopez-Sanchez, I. & Lazo, P. A. Human VRK1 is an early response gene and its loss causes a block in cell cycle progression. *PLoS One* **3**, e1642 (2008).
28. Cerutti, H. & Casas-Mollano, J. A. Histone H3 phosphorylation: Universal code or lineage specific dialects?. *Epigenetics* **4**, 71–75 (2009).
29. Klerkx, E. P., Lazo, P. A. & Askjaer, P. Emerging biological functions of the vaccinia-related kinase (VRK) family. *Histol. Histopathol.* **24**, 749–759 (2009).
30. Renbaum, P. *et al.* Spinal muscular atrophy with pontocerebellar hypoplasia is caused by a mutation in the VRK1 gene. *Am. J. Hum. Genet.* **85**, 281–289 (2009).
31. Scheeff, E. D., Eswaran, J., Bunkoczi, G., Knapp, S. & Manning, G. Structure of the pseudokinase VRK3 reveals a degraded catalytic site, a highly conserved kinase fold, and a putative regulatory binding site. *Structure* **17**, 128–138 (2009).
32. Wiebe, M. S., Nichols, R. J., Molitor, T. P., Lindgren, J. K. & Traktman, P. Mice deficient in the serine/threonine protein kinase VRK1 are infertile due to a progressive loss of spermatogonia. *Biol. Reprod.* **82**, 182–193 (2010).
33. Baek, S. H. When signaling kinases meet histones and histone modifiers in the nucleus. *Mol. Cell* **42**, 274–284 (2011).
34. Valbuena, A., Sanz-Garcia, M., Lopez-Sanchez, I., Vega, F. M. & Lazo, P. A. Roles of VRK1 as a new player in the control of biological processes required for cell division. *Cell Signal.* **23**, 1267–1272 (2011).
35. Lee, N. *et al.* Vaccinia-related kinase 1 promotes hepatocellular carcinoma by controlling the levels of cell cycle regulators associated with G1/S transition. *Oncotarget* **6**, 30130–30148 (2015).
36. Campillo-Marcos, I., Garcia-Gonzalez, R., Navarro-Carrasco, E. & Lazo, P. A. The human VRK1 chromatin kinase in cancer biology. *Cancer Lett.* **503**, 117–128 (2021).
37. Vermeulen, M. & Timmers, H. T. Grasping trimethylation of histone H3 at lysine 4. *Epigenomics* **2**, 395–406 (2010).
38. Bierne, H. Cross talk between bacteria and the host epigenetic machinery. In *Epigenetics of Infectious Diseases* (eds Doerfler, W. & Casadesús, J.) (Springer, 2017).
39. Hammond, S. L. *et al.* Mitotic phosphorylation of histone H3 threonine 80. *Cell Cycle* **13**, 440–452 (2014).
40. Carrion-Marchante, R. *et al.* DNA aptamers against vaccinia-related kinase (VRK) 1 block proliferation in MCF7 breast cancer cells. *Pharmaceuticals (Basel)* **14**, 473 (2021).
41. Shields, J. A. *et al.* VRK1 is a paralog synthetic lethal target in VRK2-methylated glioblastoma. *bioRxiv*, 2021.2012.2030.474571 (2022).
42. Hegarat, N. *et al.* Cyclin A triggers Mitosis either via the Greatwall kinase pathway or Cyclin B. *EMBO J.* **39**, e104419 (2020).
43. Peddinti, D., Memili, E. & Burgess, S. C. Proteomics-based systems biology modeling of bovine germinal vesicle stage oocyte and cumulus cell interaction. *PLoS One* **5**, e11240 (2010).
44. Manning, G., Whyte, D. B., Martinez, R., Hunter, T. & Sudarsanam, S. The protein kinase complement of the human genome. *Science* **298**, 1912–1934 (2002).
45. Nichols, R. J., Wiebe, M. S. & Traktman, P. The vaccinia-related kinases phosphorylate the N' terminus of BAF, regulating its interaction with DNA and its retention in the nucleus. *Mol. Biol. Cell* **17**, 2451–2464 (2006).
46. Park, C. H. *et al.* Protein kinase Cdelta regulates vaccinia-related kinase 1 in DNA damage-induced apoptosis. *Mol. Biol. Cell* **22**, 1398–1408 (2011).
47. Stutzer, A. *et al.* Modulations of DNA contacts by linker histones and post-translational modifications determine the mobility and modifiability of nucleosomal H3 tails. *Mol. Cell* **61**, 247–259 (2016).
48. Wang, F. *et al.* A positive feedback loop involving Haspin and Aurora B promotes CPC accumulation at centromeres in mitosis. *Curr. Biol.* **21**, 1061–1069 (2011).
49. Ghenoiu, C., Wheelock, M. S. & Funabiki, H. Autoinhibition and Polo-dependent multisite phosphorylation restrict activity of the histone H3 kinase Haspin to mitosis. *Mol. Cell* **52**, 734–745 (2013).
50. Zhou, L., Tian, X., Zhu, C., Wang, F. & Higgins, J. M. Polo-like kinase-1 triggers histone phosphorylation by Haspin in mitosis. *EMBO Rep.* **15**, 273–281 (2014).
51. Yu, F. *et al.* Aurora-A promotes the establishment of spindle assembly checkpoint by priming the Haspin-Aurora-B feedback loop in late G2 phase. *Cell Discov.* **3**, 16049 (2017).
52. Qian, J., Beullens, M., Lesage, B. & Bollen, M. Aurora B defines its own chromosomal targeting by opposing the recruitment of the phosphatase scaffold repo-man. *Curr. Biol.* **23**, 1136–1143 (2013).
53. Qian, J., Lesage, B., Beullens, M., Van Eynde, A. & Bollen, M. PP1/Repo-man dephosphorylates mitotic histone H3 at T3 and regulates chromosomal aurora B targeting. *Curr. Biol.* **21**, 766–773 (2011).
54. Vagnarelli, P. *et al.* Repo-Man coordinates chromosomal reorganization with nuclear envelope reassembly during mitotic exit. *Dev. Cell* **21**, 328–342 (2011).
55. Najmabadi, H. *et al.* Deep sequencing reveals 50 novel genes for recessive cognitive disorders. *Nature* **478**, 57–63 (2011).
56. Gonzaga-Jauregui, C. *et al.* Mutations in VRK1 associated with complex motor and sensory axonal neuropathy plus microcephaly. *JAMA Neurol.* **70**, 1491–1498 (2013).
57. Vinograd-Byk, H., Renbaum, P. & Levy-Lahad, E. Vrk1 partial knockdown in mice results in reduced brain weight and mild motor dysfunction, and indicates neuronal VRK1 target pathways. *Sci. Rep.* **8**, 11265 (2018).
58. So, J. *et al.* VRK1 is required in VRK2-methylated cancers of the nervous system. *bioRxiv*, 2021.2012.2028.474386 (2021).
59. Aihara, H. *et al.* Nucleosomal histone kinase-1 phosphorylates H2A Thr 119 during mitosis in the early Drosophila embryo. *Genes Dev.* **18**, 877–888 (2004).
60. Lancaster, O. M., Cullen, C. F. & Ohkura, H. NHK-1 phosphorylates BAF to allow karyosome formation in the Drosophila oocyte nucleus. *J. Cell Biol.* **179**, 817–824 (2007).
61. Gorjanacz, M. *et al. Caenorhabditis elegans* BAF-1 and its kinase VRK-1 participate directly in post-mitotic nuclear envelope assembly. *EMBO J.* **26**, 132–143 (2007).
62. Molitor, T. P. & Traktman, P. Depletion of the protein kinase VRK1 disrupts nuclear envelope morphology and leads to BAF retention on mitotic chromosomes. *Mol. Biol. Cell* **25**, 891–903 (2014).
63. Nikalayevich, E. & Ohkura, H. The NuRD nucleosome remodelling complex and NHK-1 kinase are required for chromosome condensation in oocytes. *J. Cell Sci.* **128**, 566–575 (2015).
64. Samwer, M. *et al.* DNA cross-bridging shapes a single nucleus from a set of mitotic chromosomes. *Cell* **170**, 956-972 e923 (2017).
65. Watson, N. A. *et al.* Kinase inhibition profiles as a tool to identify kinases for specific phosphorylation sites. *Nat. Commun.* **11**, 1684 (2020).
66. Anastassiadis, T., Deacon, S. W., Devarajan, K., Ma, H. & Peterson, J. R. Comprehensive assay of kinase catalytic activity reveals features of kinase inhibitor selectivity. *Nat. Biotechnol.* **29**, 1039–1045 (2011).
67. Gao, Y. *et al.* A broad activity screen in support of a chemogenomic map for kinase signalling research and drug discovery. *Biochem. J.* **451**, 313–328 (2013).
68. Davis, M. I. *et al.* Comprehensive analysis of kinase inhibitor selectivity. *Nat. Biotechnol.* **29**, 1046–1051 (2011).
69. Fedorov, O. *et al.* A systematic interaction map of validated kinase inhibitors with Ser/Thr kinases. *Proc. Natl. Acad. Sci. U.S.A.* **104**, 20523–20528 (2007).
70. Karakkat, J. V. *et al.* The metabolic sensor PASK is a histone 3 kinase that also regulates H3K4 methylation by associating with H3K4 MLL2 methyltransferase complex. *Nucleic Acids Res.* **47**, 10086–10103 (2019).

71. Murphy, J. M. *et al.* A robust methodology to subclassify pseudokinases based on their nucleotide-binding properties. *Biochem. J.* **457**, 323–334 (2014).
72. Nichols, R. J. & Traktman, P. Characterization of three paralogous members of the mammalian vaccinia related kinase family. *J. Biol. Chem.* **279**, 7934–7946 (2004).
73. Feizbakhsh, O. *et al.* A peak of H3T3 phosphorylation occurs in synchrony with mitosis in sea urchin early embryos. *Cells* **9**, 898 (2020).
74. Xie, J. *et al.* Histone H3 threonine phosphorylation regulates asymmetric histone inheritance in the drosophila male germline. *Cell* **163**, 920–933 (2015).
75. Fresan, U., Rodriguez-Sanchez, M. A., Reina, O., Corces, V. G. & Espinas, M. L. Haspin kinase modulates nuclear architecture and Polycomb-dependent gene silencing. *PLoS Genet.* **16**, e1008962 (2020).
76. Ashtiyani, R. K. *et al.* AtHaspin phosphorylates histone H3 at threonine 3 during mitosis and contributes to embryonic patterning in Arabidopsis. *Plant J.* **68**, 443–454 (2011).
77. Kurihara, D., Matsunaga, S., Omura, T., Higashiyama, T. & Fukui, K. Identification and characterization of plant Haspin kinase as a histone H3 threonine kinase. *BMC Plant Biol.* **11**, 73 (2011).
78. Nguyen, A. L. *et al.* Phosphorylation of threonine 3 on histone H3 by haspin kinase is required for meiosis I in mouse oocytes. *J. Cell Sci.* **127**, 5066–5078 (2014).
79. Kang, H., Park, Y. S., Cho, D. H., Kim, J. S. & Oh, J. S. Dynamics of histone H3 phosphorylation at threonine 3 during meiotic maturation in mouse oocytes. *Biochem. Biophys. Res. Commun.* **458**, 280–286 (2015).
80. Valbuena, A., Blanco, S., Vega, F. M. & Lazo, P. A. The C/H3 domain of p300 is required to protect VRK1 and VRK2 from their downregulation induced by p53. *PLoS One* **3**, e2649 (2008).
81. Kang, T. H., Park, D. Y., Kim, W. & Kim, K. T. VRK1 phosphorylates CREB and mediates CCND1 expression. *J. Cell Sci.* **121**, 3035–3041 (2008).
82. Aihara, H. *et al.* Histone H2A T120 phosphorylation promotes oncogenic transformation via upregulation of cyclin D1. *Mol. Cell* **64**, 176–188 (2016).
83. Molitor, T. P. & Traktman, P. Molecular genetic analysis of VRK1 in mammary epithelial cells: Depletion slows proliferation in vitro and tumor growth and metastasis in vivo. *Oncogenesis* **2**, e48 (2013).
84. Cullen, C. F., Brittle, A. L., Ito, T. & Ohkura, H. The conserved kinase NHK-1 is essential for mitotic progression and unifying acentrosomal meiotic spindles in *Drosophila melanogaster*. *J. Cell Biol.* **171**, 593–602 (2005).
85. Schober, C. S., Aydiner, F., Booth, C. J., Seli, E. & Reinke, V. The kinase VRK1 is required for normal meiotic progression in mammalian oogenesis. *Mech. Dev.* **128**, 178–190 (2011).
86. Ivanovska, I., Khandan, T., Ito, T. & Orr-Weaver, T. L. A histone code in meiosis: The histone kinase, NHK-1, is required for proper chromosomal architecture in *Drosophila* oocytes. *Genes Dev.* **19**, 2571–2582 (2005).
87. McCracken, A. & Locke, J. Mutations in CG8878, a novel putative protein kinase, enhance P element dependent silencing (PDS) and position effect variegation (PEV) in Drosophila melanogaster. *PLoS One* **9**, e71695 (2014).
88. Brittle, A. L., Nanba, Y., Ito, T. & Ohkura, H. Concerted action of Aurora B, Polo and NHK-1 kinases in centromere-specific histone 2A phosphorylation. *Exp. Cell Res.* **313**, 2780–2785 (2007).
89. Ricke, R. M., Jeganathan, K. B., Malureanu, L., Harrison, A. M. & van Deursen, J. M. Bub1 kinase activity drives error correction and mitotic checkpoint control but not tumor suppression. *J. Cell Biol.* **199**, 931–949 (2012).
90. Maeda, K. *et al.* Defects in centromeric/pericentromeric histone H2A T120 phosphorylation by hBUB1 cause chromosome mis-segregation producing multinucleated cells. *Genes Cells* **23**, 828–838 (2018).
91. Park, S. *et al.* VRK-1 extends life span by activation of AMPK via phosphorylation. *Sci. Adv.* **6**, eaaw7824 (2020).
92. Quadri, R. *et al.* Phosphorylation of H3-Thr3 by Haspin is required for primary cilia regulation. *Int. J. Mol. Sci.* **22**, 7753 (2021).
93. Casas-Mollano, J. A., Jeong, B. R., Xu, J., Moriyama, H. & Cerutti, H. The MUT9p kinase phosphorylates histone H3 threonine 3 and is necessary for heritable epigenetic silencing in *Chlamydomonas*. *Proc. Natl. Acad. Sci. U.S.A.* **105**, 6486–6491 (2008).
94. Wang, Z. *et al.* Osmotic stress induces phosphorylation of histone H3 at threonine 3 in pericentromeric regions of *Arabidopsis thaliana*. *Proc. Natl. Acad. Sci. U.S.A.* **112**, 8487–8492 (2015).
95. Schindelin, J. *et al.* Fiji: An open-source platform for biological-image analysis. *Nat. Methods* **9**, 676–682 (2012).
96. Mon, A. M., MacKinnon, A. C. Jr. & Traktman, P. Overexpression of the VRK1 kinase, which is associated with breast cancer, induces a mesenchymal to epithelial transition in mammary epithelial cells. *PLoS One* **13**, e0203397 (2018).
97. Umland, T. C., Wei, S. Q., Craigie, R. & Davies, D. R. Structural basis of DNA bridging by barrier-to-autointegration factor. *Biochemistry* **39**, 9130–9138 (2000).
98. Samson, C. *et al.* Structural analysis of the ternary complex between lamin A/C, BAF and emerin identifies an interface disrupted in autosomal recessive progeroid diseases. *Nucleic Acids Res.* **46**, 10460–10473 (2018).
99. Elkins, J. M. *et al.* Comprehensive characterization of the Published Kinase Inhibitor Set. *Nat. Biotechnol.* **34**, 95–103 (2016).

Acknowledgements

The PKIS1 library was supplied by GlaxoSmithKline LLC and the Structural Genomics Consortium under an open access Material Transfer and Trust Agreement: http://www.sgc-unc.org. The authors gratefully acknowledge the Newcastle University BioImaging Unit for their support and assistance in this work. This study was funded by a Wellcome Trust Investigator Award (106951/Z/15/Z), a Royal Society Wolfson Research Merit Award, and an MRC Confidence in Concept award to J.M.G.H., and a Royal Society Newton Advanced Fellowship (NA140075) to F.W. and J.M.G.H. For the purpose of open access, the author has applied a CC BY public copyright licence to any Author Accepted Manuscript version arising from this submission.

Author contributions

T.N.C. and R.J.H. designed, conducted and analysed multiple experiments; S.K.M. carried out KiPIK screens; N.A.W. conducted KiPIK and RNAi screens; C.T. conducted ELISA and RNAi experiments; A.M.M. produced recombinant forms of VRK1 and BAF and conducted radioactive kinase assays; P.T. supervised A.M.M. and provided BAF S4ph antibodies; F.W. provided Haspin KO HeLa cells; A.M. produced recombinant BAF under the supervision of S.Z.J.; J.M.G.H. supervised the project, analysed data, and wrote the manuscript draft. All authors made comments on the manuscript.

Competing interests

Nikolaus Watson and Jonathan Higgins are inventors on international patent filing WO/2020/225535 "Kinase screening assays" that covers the KiPIK procedure. The other authors declare that they have no conflict of interest.

Additional information

Supplementary Information The online version contains supplementary material available at https://doi.org/10.1038/s41598-022-15339-8.

Correspondence and requests for materials should be addressed to J.M.G.H.

Reprints and permissions information is available at www.nature.com/reprints.

Publisher's note Springer Nature remains neutral with regard to jurisdictional claims in published maps and institutional affiliations.